

Neutron-Induced Reactions in Third and Fourth Shell Nuclei*

F. L. HASSLER† AND R. A. PECK, JR.
Brown University, Providence, Rhode Island

(Received March 30, 1961)

A counter telescope and scintillation spectrometer were used to obtain spectra and angular distributions (0° to 150° at 30° intervals) of the (n,p) reactions at 14 Mev on the targets Mg, Al, Si, P, S, Ti, Fe, Co, Ni, and Zn. Contributions of (n,d) have been separated by two independent experimental methods, and direct interaction contributions by the criterion of angular asymmetry. The residual yield has been analyzed to give values of temperature (accuracy about 10%) and spin-dependence parameters (lower limits), which compare reasonably with independent values based on collected level information. Fractions of direct interaction are quite well described by the model of Brown and Muirhead, and total cross sections are consistent with available determinations by other methods. Angular distributions of strong (n,d) ground-state groups from P and S have the appropriate pickup forms.

THE angular anisotropy of particle emission in nuclear reactions passing through the continuum region of a compound nucleus is closely related to the distribution of nuclear states among angular momenta. The formal theory of reactions^{1,2} shows that a necessary prerequisite for isotropy, as also for independence of formation and decay processes at an excitation U , is a factorable level-density function of the form

$$\rho_J(U) = (2J+1)\rho_0(U). \quad (1)$$

When a deviation from this form of J dependence is represented by the relation^{3,4}

$$\rho_J(U) = \rho_0(U)(2J+1) \exp[-J(J+1)/2\sigma^2], \quad (2)$$

the parameter σ appears also as a factor in the coefficient of anisotropy (A) of the angular distribution,^{2,4} expressed in the form $(1+A \cos^2\theta)$.

Insofar as the parameter A is excitation-dependent, it is related not only to the angular anisotropy but also to the temperature describing the smoothed spectrum. Two different temperature parameters are relevant, the normal one (T) related to the level density by

$$\frac{1}{T} = \frac{d}{dU} \ln \rho(U), \quad (3)$$

and an integral analog⁵ (τ),

$$\frac{1}{\tau} = \frac{d}{dU} \ln N(U) = \frac{\rho(U)}{N(U)}, \quad (4)$$

similarly related to $N(U)$, the total number of states below the excitation U . The first (T) can be determined

from a semi-empirical formulation of level densities; for comparison with the present work, that of Newton has been used.⁶ This is based on the form (1) and gives the excitation dependence

$$\rho_0 \propto (2U+3t)^{-2} \times \exp\{-2[(\pi^2/3)\alpha(\bar{j}_N + \bar{j}_Z + 1)A^{\frac{1}{2}}U]^{\frac{1}{2}}\}, \quad (5a)$$

with

$$t = [(3U/\pi^2)\alpha(\bar{j}_N + \bar{j}_Z + 1)A^{\frac{1}{2}}U]^{\frac{1}{2}}. \quad (5b)$$

For nuclei for which complete level data exist, the second temperature parameter (τ) is determined directly from its definition.⁵ A difference between the two measures a deviation of the level-density function from the simple exponential form.

The spin-dependence parameter σ can be estimated independently of angular distributions if complete level-density data are available. This determination depends on the temperature parameter τ , the relation being

$$4\sigma^2\tau \approx N(U)/\rho_0(U), \quad (6)$$

$N(U)$ being determined by direct counting and $\rho_0(U)$, the density of spin-zero states, from slow-neutron resonance data. Determination of σ from angular anisotropy does not require a temperature value.

In the experiment reported, energy spectra and angular distributions of protons and deuterons were observed following the neutron bombardment of Mg, Al, Si, P, S, Ti, Fe, Co, Ni, and Zn. The object has been to isolate those parts of the distributions corresponding to continuum (n,p) processes and thus to survey the statistical parameters identified above in the third and fourth atomic shells.

EXPERIMENTAL

Neutrons of 14.4 Mev were produced by the D+T reaction in a 175-kv Cockcroft-Walton accelerator.⁷ Target geometry confined the incident neutrons to a cone of half-angle 8° and axis perpendicular to the deuteron beam, the corresponding neutron energy

* Supported in part by the U. S. Atomic Energy Commission.
† Submitted in partial fulfillment of the requirements for the Ph.D. degree at Brown University. Present address: Mitre Corporation, Bedford, Massachusetts.

¹ A. M. Lane and R. G. Thomas, *Revs. Modern Phys.* **30**, 257 (1958).

² A. C. Douglas and N. MacDonald, *Nuclear Phys.* **13**, 382 (1959).

³ C. Bloch, *Phys. Rev.* **93**, 1094 (1954).

⁴ T. Ericson and V. Strutinski, *Nuclear Phys.* **8**, 284 (1958); **9**, 689 (1958/1959).

⁵ T. Ericson, *Nuclear Phys.* **11**, 481 (1959).

⁶ T. D. Newton, *Can. J. Phys.* **34**, 804 (1956).

⁷ R. A. Peck, Jr., and H. P. Eubank, *Rev. Sci. Instr.* **26**, 444 (1955).

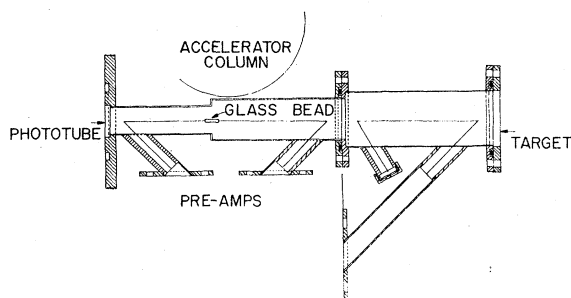


FIG. 1. Cross section of counter telescope.

spread (± 0.2 Mev) being confirmed by resolution studies. Beam currents ranging between 0.1 and 1.0 ma were employed to maintain production rates of approximately 5×10^9 neutrons/sec. The neutron flux was continuously monitored by a BF_3 "long counter," calibrated before and after each run with a Ra-Be source. The observed mean variation of monitor sensitivity in a run was 3.7%.

The most severe experimental problem was observing legitimate events occurring at rates of order 1 per sec in the presence of a background counting rate in the energy detector of about 10^4 per sec. The cylindrical walls of the counter telescope (Fig. 1) were of brass machined to 0.025-in. thickness and lined with lead 14 Mev thick

to protons. Three gas proportional counters were utilized to reduce the accidental coincidence rate and to provide a restrictive geometry minimizing the number of events triggering all three counters but not originating in the target. The target was 1 in. in diameter, 3.5 in. from the neutron source and 7 in. from the energy detector, a CsI crystal 0.534 in. in diameter and 0.0275 in. thick cemented to the face of an RCA 6342A phototube. The maximum spread of reaction angle permitted by this system is about $\pm 12^\circ$ on the average. At the beginning of each run the counters were freshly filled with 12.5 cm Hg of argon plus 5% CO_2 and mounted on a stand permitting rotation of the telescope assembly about a vertical axis through the front window, to which the target was affixed. Energy spectra spread over 20 channels were observed at 30° intervals from 0° to 150° .

Signals from the three gas counters were passed through independent preamplifiers, amplifiers and discriminators to the coincidence circuit which, if the separate gas pulses exceeded the reference voltages of the low-level discriminators and were coincident within $1 \mu\text{sec}$, generated a 15-v, 2- μsec gate pulse opening the 20-channel pulse-height analyzer to which the amplified crystal pulse was led. All crystal events occurring within the gate pulse length were registered. With this arrangement the ratio of legitimate to background counting rates ranged between 3:1 and 1:4.

The best energy resolution observed was 8%, of which about half can be attributed to the finite channel width. Each spectrum was corrected for the nonuniform channel width resulting from nonlinear absorptive energy loss in the telescope material and half the target thickness.

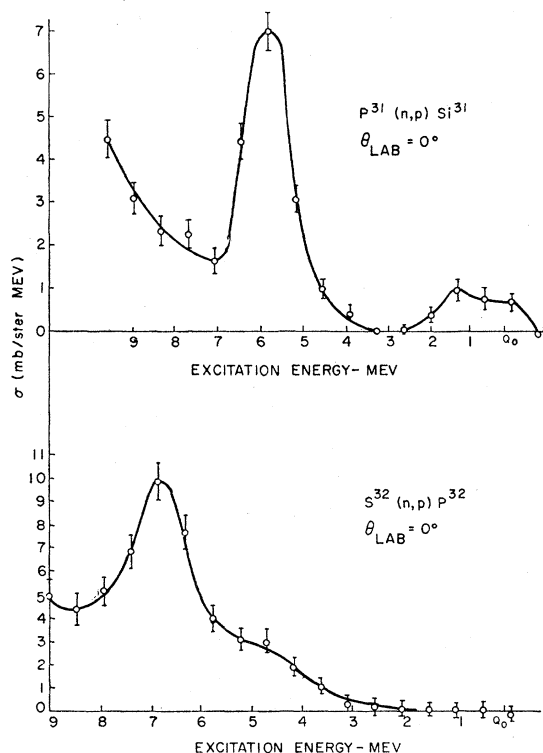


FIG. 2. Charged-particle spectra after background removal and correction for energy loss in absorbers. Proton energy is in laboratory system; statistical bars show standard deviations. Prominent peaks are (n,d) ground-state groups.

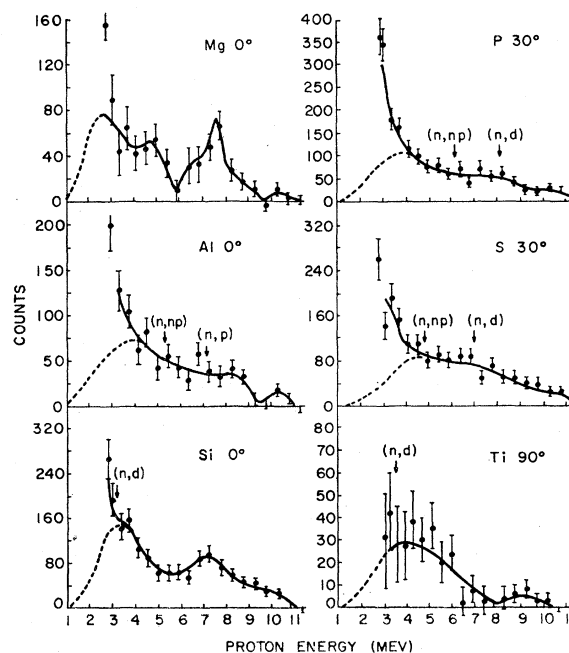


FIG. 3. Same as Fig. 2. Deuterons are suppressed.

SPECTRA

Preliminary measurements⁸ indicated the likelihood of strong (n,d) ground-state groups in several of the spectra, particularly P and S (Fig. 2). Deuteron contributions were extracted by two independent methods. (1) Independent observation of the proton and deuteron detection efficiencies as functions of gas multiplication in the proportional counters permitted the two to be separated in the experimental spectra by variation of gas counter voltages. (2) It was observed that the proton angular distributions on each side of the pronounced deuteron peaks were similar slowly varying functions of reaction angle. Normalizing this shape to fit the particle yield within the energy range of the (n,d) peak at large angles, where the pickup reaction is expected to contribute little, it was possible to extract the presumed proton contribution at smaller angles. Results of the two approaches to deuteron separation were in good agreement.

Representative spectra (0°) are shown in Figs. 2-4, after deuteron removal. Range absorption in target and telescope precludes the contribution of (n,α) and (n,t) events in the main. From the proton yields remaining after extraction of deuteron contributions, the presumed compound nucleus yield was isolated on the usual basis of symmetry about 90° . While it is recognized⁹ that this simple criterion is not rigorous, it has yet to be shown that it is not a fair guide for a survey such as this, nor was a rigorous discrimination feasible in this experiment. Any (n,np) contributions which occur are necessarily included in the yields which are analyzed. Dotted lines on the energy spectra (Figs. 3, 4) show the (n,p) shapes obtained by linear extrapolation of the semi-logarithmic spectra to low energies.

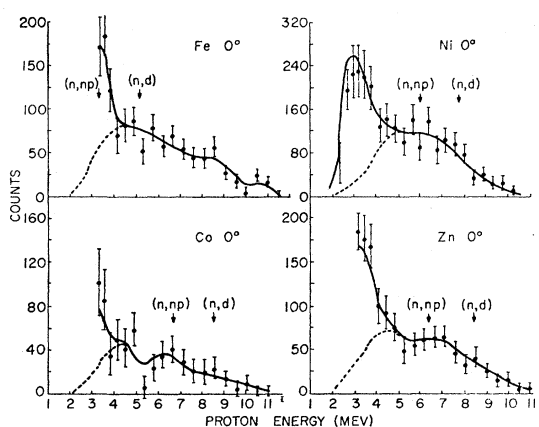


FIG. 4. Same as Fig. 2. Deuterons are suppressed.

⁸ H. P. Eubank, M. R. Zatzick, and F. L. Hassler, *Bull. Am. Phys. Soc.* **4**, 287 (1959).

⁹ T. Ericson, *Proceedings of the International Conference on Nuclear Structure, Kingston*, edited by D. A. Bromley and E. W. Vogt (University of Toronto Press, Toronto, Canada, 1960), p. 697 ff.

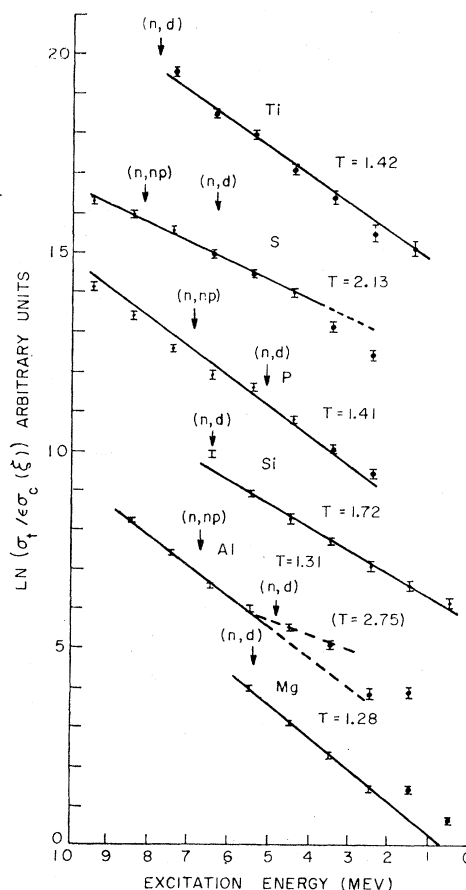


FIG. 5. Conventional statistical theory plot of integrated spectra. Vertical arrows mark maximum possible energies for reactions as labeled. Dashed lines are extrapolations of linear temperature plots to regions where other reaction mechanisms may occur.

The yields of successive 1-Mev segments of spectra, integrated over the full laboratory solid angle and weighted with the usual compound nucleus factors^{10,11} are displayed semilogarithmically in Figs. 5 and 6. The corresponding temperature parameters are entered in Table I, together with τ values derived from known level schemes¹² and conventional T values derived from the semiempirical level density expression (5). In this equation the parameter α has been adjusted, as is required to allow for a J dependence of level density differing from (1). The empirical value from this experiment is 27% larger than that⁶ determined from slow-neutron resonance data.

¹⁰ J. M. Blatt and V. F. Weisskopf, *Theoretical Nuclear Physics* (John Wiley & Sons, Inc., New York, 1952), p. 367.

¹¹ M. Shapiro, *Phys. Rev.* **90**, 170 (1953).

¹² A. W. Dalton, S. Hinds, and G. Parry, *Proc. Phys. Soc. (London)* **A70**, 586 (1957); P. M. Endt and C. M. Braams, *Revs. Modern Phys.* **29**, 683 (1957); R. P. de Figueiredo, M. Mazari, and W. W. Buechner, *Phys. Rev.* **112**, 873 (1958); G. M. Foglesong and D. G. Foxwell, *ibid.* **96**, 1001 (1954); L. W. Green, A. J. Smith, W. W. Buechner, and M. Mazari, *ibid.* **108**, 841 (1957); S. Hinds, R. Middleton, and G. Parry, *Proc. Phys. Soc. (London)* **A71**, 49 (1949); A. Sperduto, Massachusetts Institute of Technology L. N. S. Progress Report, November, 1957 (unpublished).

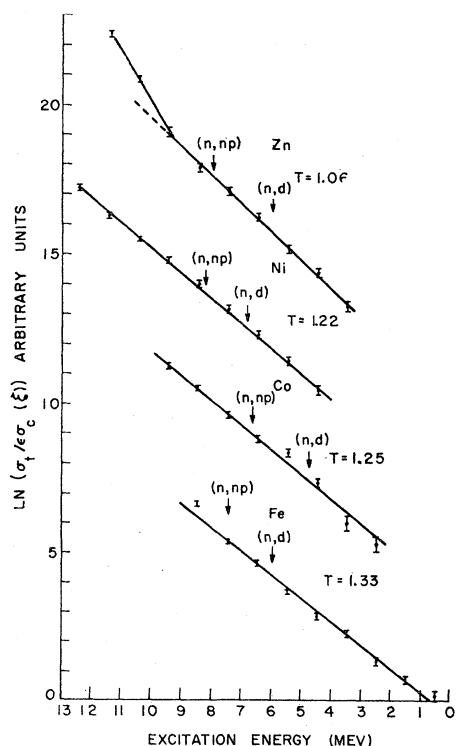


FIG. 6. Same as Fig. 5.

Experimental temperature values match τ in five cases (Mg, Al, Si, Co, Zn) and T in three (Fe, Co, Ni). It is interesting that the three cases of disagreement with both parameters (P, S, Ti) are neighbors in the series studied, and a residual shell effect may be indicated. For Mg, Al, and Zn the statistical plots suggest two temperatures for different excitation ranges, confirming a recent observation¹³ in the case of Zn and for Mg reflected also in the neutron data from which the theoretical τ is determined.⁵

TABLE I. Temperature parameters^a (MeV).

Target	T^b	T^c	τ^d
Mg	1.28 ± 0.07	1.95	$\begin{cases} 1.7 \\ 1.98 \end{cases}$
Al	$\begin{cases} 1.31 \pm 0.08 \\ (2.8) \end{cases}$	2.21	$\begin{cases} 1.4 \\ 2.5 \end{cases}$
Si	1.72 ± 0.07	2.21	1.79
P	1.4 ± 0.10	1.95	1.98
S	2.13 ± 0.10	2.70	3.01
Ti	1.42 ± 0.08	1.06	
Fe	1.33 ± 0.08	1.30	1.14
Co	1.25 ± 0.09	1.21	1.26
Ni	1.22 ± 0.08	1.21	1.82
Zn	1.06 ± 0.10	1.28	1.16

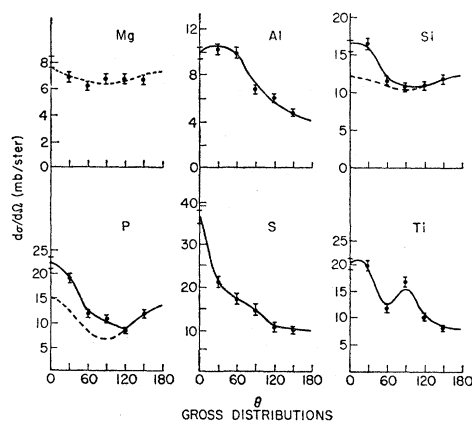
^a Defined in introduction.^b From spectra, this experiment.^c From Eq. (5).^d Reference 12.

FIG. 7. Angular distributions of entire spectra. Dashed curves indicate compound nucleus contribution assumed. Angles are in laboratory system.

ANGULAR DISTRIBUTIONS

Figures 7 and 8 show the angular distributions of total proton yields, summed over energy. From the five curves giving some indication of an increase in cross section with angle past 90° the anisotropy coefficient A (in a fit to $1 + A \cos^2 \theta$) was estimated, and from it the spin-dependence parameter σ .

The values of σ are listed in Table II. Ranges shown for the comparison values reflect the range of possible values of τ , which is required for the translation of level data into σ values [Eq. (6)]. Only upper limits to anisotropies can be assigned in this experiment, isotropy within the standard deviations (past 90°) being possible

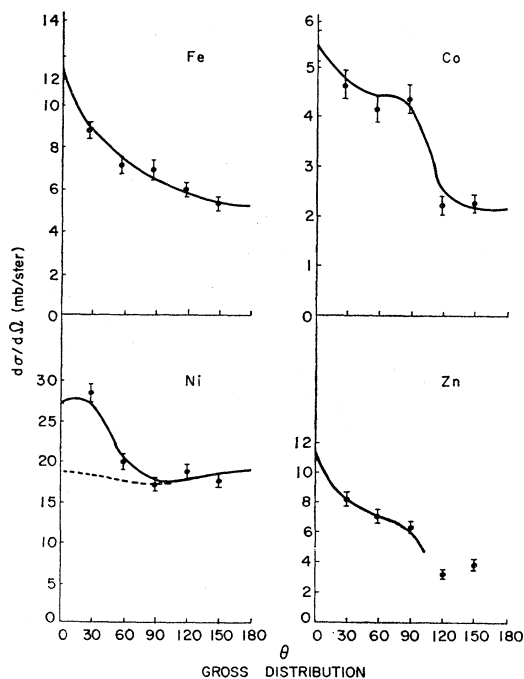


FIG. 8. Same as Fig. 7.

¹³ A. H. Armstrong and L. Rosen, Nuclear Phys. 19, 40 (1960).

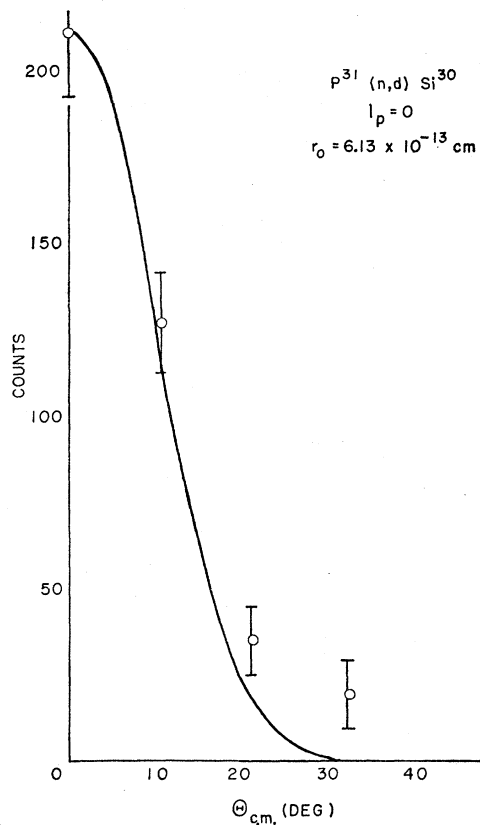


FIG. 9. Angular distribution of (n,d) ground-state transition with fitted Butler curve. Angles are in center-of-mass system.

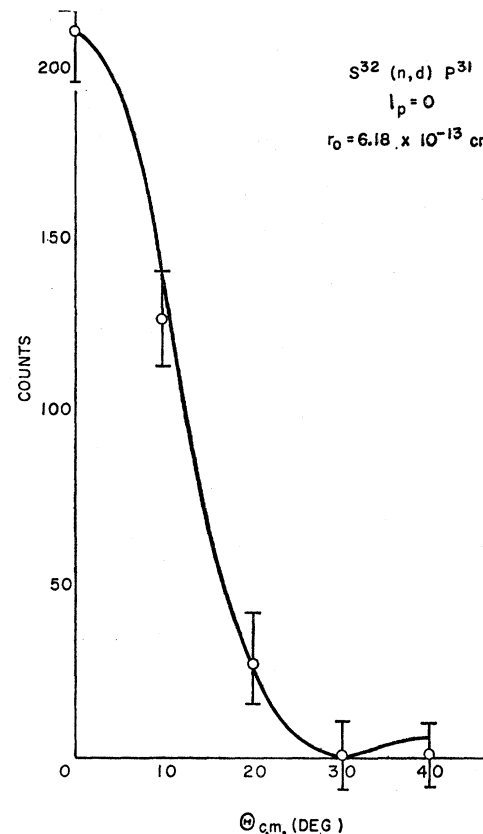


FIG. 10. Same as Fig. 9.

in all cases. While no comparison value is available for phosphorus, the behavior of this nucleus is observed to be generally quite similar to that of sulfur. The σ value deduced for sulfur from level data⁶ is the lowest of the nuclides studied.

Figures 9 and 10 show the angular distributions of the two particularly strong (n,d) ground-state groups. Both phosphorus and sulfur exhibit pick up distributions characteristic of $l=0$ transitions, as expected from shell-model considerations, and the interaction radii are reasonable.

CROSS SECTIONS

Absolute cross sections were determined by reference to the differential $n-p$ scattering cross section at 0°

TABLE II. Spin dispersion parameters, σ .¹⁴

	This experiment	Comparison	Reference
Mg	>1.5	2.4–5.2	6
Si	≥ 1.4	1.7	14
		2.8–3.9	6
P	0.9–1.3		
Ni	≥ 2.4	1.3–2.0	6
Zn	>1.2	2.3–6.0	6

¹⁴ C. T. Hibdon, Bull. Am. Phys. Soc. **3**, 48 (1958).

(polyethylene radiator). Total cross sections derived from the observed angular distributions are shown in the top two lines of Table III; the (n,np) yield, where recorded, has been assumed isotropic. The third line identifies the minimum (cutoff) proton energy to which the cross sections refer, and the fourth line the fraction of total cross section which was identified with direct interaction processes on the basis of angular anisotropy. In the lower half of the table are other determinations of the total cross sections,¹⁵ for the most part from activation measurements and hence expected to exceed the determinations of this experiment. The last line shows the estimates of the fraction of direct interaction processes computed from the successive scattering model of Brown and Muirhead.¹⁶

The total cross sections are in most cases reasonably consistent with earlier determinations. The principal

¹⁵ D. L. Allan, Proc. Phys. Soc. (London) **A70**, 195 (1957); G. Brown, G. C. Morrison, and W. T. Morton, Phil. Mag. **2**, 785 (1957); A. V. Cohen and P. H. White, Nuclear Phys. **1**, 73 (1957); H. P. Eubank, R. A. Peck, Jr., and F. L. Hassler, *ibid.* **9**, 273 (1958/1959); S. G. Forbes, Phys. Rev. **88**, 1309 (1952); J. A. Grundl, R. L. Henkel, and B. L. Perkins, *ibid.* **109**, 425 (1958); R. K. Haling, R. A. Peck, Jr., and H. P. Eubank, *ibid.* **106**, 971 (1957); C. S. Khurana and H. S. Hans, Nuclear Phys. **13**, 88 (1959); E. B. Paul and R. L. Clarke, Can. J. Phys. **31**, 267 (1953); L. Rosen and A. H. Armstrong, Bull. Am. Phys. Soc. **1**, 224 (1956).

¹⁶ G. Brown and H. Muirhead, Phil. Mag. **2**, 473 (1957).

TABLE III. Total cross sections.

Target	$\sigma(n,p)$ (mb)	This experiment			Comparison values		
		$\sigma(n,np)$ (mb)	E_{\min} (Mev)	D.I. ^a (%)	$\sigma(n,p)^b$ (mb)	$\sigma(n,np)^b$ (mb)	D.I. ^{a,c} (%)
Mg	88±9	17±6	3.0	3	155	60	22-50
Al	93±10		2.8	45	81		55
Si	160±16	70±14	2.9	10	225		17
P	155±16		2.9	24	85		50
S	206±21	73±15	2.8	37	369		23
Ti	35±4		3.7	40	~81	124	23
Fe	102±10	~11	2.8	26	124		47
Co	48±5		3.0	39			
Ni	255±26	240±50	1.5	13			14
Zn	170±20 ^d		2.2	43	>300 ^d		35

^a Fraction of (n,p) yield attributed to direct interaction (D.I.).^b Reference 15.^c Reference 16.^d Including (n,np) .

exceptions are phosphorus, for which the high value of this experiment is probably due to incomplete separation of (n,np) contributions, and zinc, for which interpretation is complicated by the number of isotopes of significant abundance. The Brown-Muirhead analysis reproduces the observed fractions of direct interaction contribution reasonably well, and would probably do so better if carried out with a shell-dependent level density

formula such as Newton's instead of the smoothly A -dependent one employed.

ACKNOWLEDGMENTS

The collaboration of Professor H. P. Eubank in the early phases of the study is gratefully acknowledged, and that of M. R. Zatzick in the design and construction of the late versions of the detection electronics.